2015

Heating Based Model Analysis for Explosive Emission Intitiation at Metal Cathodes

A. Majzoobi
Old Dominion University, amajz001@odu.edu

R. P. Joshi

A. Neuber

J. Dickens

Original Publication Citation

Majzoobi, A., Joshi, R.P., Neuber, A., & Dickens, J. (2015). Heating based model analysis for explosive emission initiation at metal cathodes. *AIP Advances, 5*(12), 1-7. doi: 10.1063/1.4939569

Heating based model analysis for explosive emission initiation at metal cathodes

A. Majzoobi,[1] R. P. Joshi,[2,a] A. Neuber,[2] and J. Dickens[2]
[1]*Department of Electrical and Computer Engineering, Old Dominion University, Norfolk, VA 23529, U.S.A.*
[2]*Department of Electrical and Computer Engineering, Texas Tech University, Lubbock, TX 79409, U.S.A.*

(Received 13 November 2015; accepted 21 December 2015; published online 31 December 2015)

This contribution presents a model analysis for the initiation of explosive emission; a phenomena that is observed at cathode surfaces under high current densities. Here, localized heating is quantitatively evaluated on ultrashort time scales as a potential mechanism that initiates explosive emission, based on a two-temperature, relaxation time model. Our calculations demonstrate a strong production of nonequilibrium phonons, ultimately leading to localized melting. Temperatures are predicted to reach the cathode melting point over nanosecond times within the first few monolayers of the protrusion. This result is in keeping with the temporal scales observed experimentally for the initiation of explosive emission. [http://dx.doi.org/10.1063/1.4939569]

I. INTRODUCTION

Electron emission from cathodes can provide high current densities (several kA/cm^2) for a variety of applications such as high power microwave generation,[1–3] free electron lasers,[4] pumping of excimer lasers,[5] for surface modifications and material processing,[6,7] and in vacuum electronics.[8,9] In this high voltage context, explosive electron emission has been reported.[10–13] A simple, qualitative explanation for initiation of the explosive emission is that an applied external voltage creates high electric fields (in the 10^7–10^8 V/cm range) at cathode micro-protrusions. However to the best of our knowledge, the mechanistic details have not been thoroughly probed, nor have analyses focused on the ultrashort time scales.

For explosive emission, the current density may reach values of 10^9 A/cm^2 or higher.[14,15] At these extreme localized, nonequilibrium situations, two important aspects need to be carefully considered: (i) strong electric fields and high temperature gradients that could exist at the cathode surface. The former would likely originate from micro-protrusions on the cathode surface leading to strong field enhancements, and also have contributions from ions that may be in close vicinity of a cathode emission site, (ii) the intense fields and thermal gradients would cause significant departure of both the electron *and* phonon distribution functions from their equilibrium values. A highly nonequilibrium electric distribution, for instance, would channel energy into the lattice phonons and rapidly increase the cathode temperature, an idea discussed decades ago by Paranjape et al.[16] (iii) Finally, reductions in thermal conductivity at the localized microstructures (e.g., nano-protrusions) due to reduced dimensionality[17,18] would add to the intensity and speed of material heating.

The overall process of explosive emission is complex. It likely involves stochastic initiations at nano-protuberance over the cathode surface which function as strong field enhancement sites; ionization of vapors that further enhance local electric fields; subsequent quenching of a site as material is explosively blown away changing the micro-geometry; and the creation of new emissive sites as emitted ions approach neighboring sites. Here we merely present a simple, physics-based

[a]email: ravi.joshi@ttu.edu

quantitative analyses of the early initiation process which is known to occur over nanosecond scales, and modestly focus on the quantitative thermal aspects. We assume the hot-electrons at cathode tips produce non-equilibrium phonons that ultimately leads to localized melting and mass ejection. It is entirely possible that the presence of ions near the emitting surface could lower and thin the potential barrier, thereby enhancing cathode currents. However, a long-duration, self-consistent inclusion of dynamic many-body, localized effects are beyond the present scope. Our analysis includes the time-evolution of temperatures at the cathode surface. The melting point is predicted to be reached on the order of a few tens of nanoseconds, in keeping with time-scales observed for the explosive emission phenomenon.

II. MODEL ANALYSIS

Our discussion of the mathematical model given in this section revolves around the following overall process sequence hypothesized for the initiation of explosive emission: (a) initial existence of random nano-protrusions at the cathode surface that leads to strong localized electric field enhancements. (b) Electron emission from such sharp corners and high-field points on the surface. (c) This leads to material heating in the neighborhood of the emission point due to energy transfer to the lattice via electron-phonon interactions. Thus, hot electrons driven by the electric field, and arriving from the metal base to the cathode surface, create nonequilibrium phonons with effective temperatures that depend on details of the wavevector-dependent, electron-phonon interactions, and the anharmonic phonon-phonon relaxation processes. (d) Localized cathode heating can ultimately produce material ejection from cathode tips due to vaporization at high local temperatures, an aspect that has been observed in experiments.[19,20] (f) Material ejection dynamically alters the emitter shape and aspect ratio. This would probably change the field distribution at the surface, and could quench or smoothen nano-emissions at some locations, while initiating new localized sources of emission at different sites (e.g., along the rim of a newly formed crater). Thus dynamic, random, nucleation sites for emission can be expected, and have indeed been observed experimentally.[11] (g) The presence of positive ions from the ejected material would work to enhance the fields, especially at small distances from the cathode. This field enhancement, coupled with ion-induced barrier thinning and lowering,[21] would work to continue the process.

For a protruding ridge as may likely exist on the surface of an emitting cathode, the field enhancement factor can easily be obtained through conformal mapping techniques.[22,23] Details have been discussed by our group[24,25] and field enhancements by factors in excess of 10^3 shown to result for an emitter height of 10 μm and a 20 nm width. Furthermore, the presence of an ion (whether due to a separate material ejection and its subsequent ionization, or in the plasma surrounding the cathode), would alter the surface electric fields and lower the barrier for electron tunneling. This notion of ion-induced field enhancements is well known.[21,26,27]

The above qualitative assertion is that high fields at nano-protrusions could be established and lead to strong electron emission currents under high biasing. The role of Joule heating due to such currents, which is the main focus of this contribution, is discussed next. Energy gained by electrons from the electric field, shifts their distribution to high energies. This excess energy is transferred to the lattice due to electron-phonon collisions, which creates "hot/nonequilibrium" phonons over time. Here we use the classical two-temperature model[28–30] to analyze the problem which assigns different temperatures to electrons (T_e) and phonons (T_L). This model has more recently been applied to study electron-phonon coupling in pulsed irradiated metal films.[31] The electron-electron interactions are assumed to be sufficiently strong to ensure a heated-drifted Maxwellian electron distribution within the metallic cathode. The time-dependent evolution can then be expressed in terms of the following coupled equations:

$$C_e \frac{dT_e}{dt} = \frac{E^2}{\rho} - \sum_{q,j} \hbar\omega(q)\left[\frac{N_j(q,T_e) - N_j(q)}{\tau_{e-ph}(q)}\right], \tag{1a}$$

$$\frac{\delta N_j(q)}{\delta t} = \frac{N_j(q,T_e) - N_j(q)}{\tau^j_{e-ph}(q)} + \frac{N_j(q,T_0) - N_j(q)}{\tau^j_x}, \tag{1b}$$

where T_e represents the electron temperature, $N_j(q,T_e)$ is the phonon population at wavevector q at the electron temperature, the j^{th} mode represents either a longitudinal optical (LO) or transverse optical (TO) phonon, ρ is the metal resistivity, ω is the wavevector dependent phonon frequency, $C_e[= \pi^2 nkT_e/(2T_F)]$ is the electron specific heat, T_F the Fermi temperature, and T_0 the ambient temperature. Also, $\tau^j_{e-ph}(q)$ and $\tau^j_x(q)$ are the characteristic times for electron-phonon scattering and phonon-phonon (decay) interactions. The term E^2/ρ in Eqn. (1a) denotes a heat source. The coupling between the two sub-systems (electron and phonon) works to drive the system towards $T_e \sim T_L$. From the time-dependent phonon distribution $N_j(q,T_L)$, the phonon temperature $T_L(t)$ can be determined via the Bose-Einstein distribution function as: $N_j(q,T_L) = 1/[exp(\hbar\omega)/(kT_L) - 1]$. The electron-phonon scattering rate $\tau^j_{e-ph}(q)$ in Eqn. (1b) is given by:[32]

$$\tau^j_{e-ph}(q) = \Xi^2 m^2 q/(2\pi\hbar^3 \rho_M), \tag{2}$$

where Ξ is the deformation potential, m the electron mass, and ρ_M the metal density. Finally, $\tau^j_x(q) = 1.4285\times10^{39}\, q^{-5}$ second.[33] For a typical metal electrode (e.g., a copper cathode) one would have the following representative values: Ξ = 3.77 eV, $\rho_M = 8.96\times10^3$ Kg/m^3, $\hbar\omega$ = 24.8 meV, $m = 9.1\times10^{-31}$ Kg, and $C_e = 70.868\ T_e$. For simplicity only the longitudinal optical (LO) phonon energy $\hbar\omega$ has been considered, though other modes such as the transverse optical (TO) modes would exist and contribute as well. Strictly, the resistivity ρ depends on the temperature due to the electron-phonon interactions. For example, the resistivity of metals (assuming pure materials without any impurities or imperfections) is expressed by the well-known Bloch-Gruneisen expression.[34–37] As a result, the resistivity scales with temperature T (in degrees Kelvin) as T^5 at low temperatures and varies linearly at high temperatures. In the case for copper, values of resistivity have been extensively studied and reported by Matula.[35] So for example, a resistivity of $1.723\text{x}10^{-8}$ Ωm at 300° K and a value of $8.62\text{x}10^{-8}$ Ωm at 1200° K were reported. A curve fit to the values reported was used to incorporate a temperature-dependent resistivity in the present calculations.

III. SIMULATION RESULTS AND DISCUSSIONS

The role of electron heating and energy transfer to the phonon system leading to the formation of "hot phonons" was probed through numerical simulations. Figures 1(a) and 1(b) show the phonon population as a function of wavevector taking a copper electrode as an example, at two different electric fields of 2×10^3 V/m and 4×10^3 V/m. These chosen fields are much lower in amplitude as compared to the enhanced values outside the cathode. This reduction would result from screening within the cathode. For a copper electrode, the electron density "n" is about 8.5×10^{22} cm^{-3}, which yields a Thomas-Fermi screening length "r_{TF}" of about 0.55 Å. Hence, for spatial distances of about 0.8 nm or lower, the electric fields near the surface of the protrusion would be well above 2×10^3 V/m, but would fall to much lower values deeper into the metal. The four simulated curves in each figure shown correspond to snapshots at time instants of 1ns, 2ns, 4ns and 8 ns. As might be expected, the phonon distributions grow larger with time as energy from the electrons is continually transferred to the phonons. Transforming the phonon distributions into effective temperature leads to the temporal evolution of $T_L(t)$. The results for $T_L(t)$ are shown in Figs. 2(a) and 2(b) at two different phonon wavevectors of $q = 5\times10^7$m^{-1} and $q = 10^9$ m^{-1}, respectively. Each figure shows three curves at the electric fields of 2×10^3 V/m, 3×10^3 V/m, and 4×10^3 V/m. In all cases, the effective temperature starts at the ambient value of 300 K, but slowly increases over time. As may be expected, the fastest rise in temperature occurs at the highest electric field value due to the largest value of the heat source term. Based on a melting temperature of ~ 1358K for copper, melting is predicted to occur at roughly around 25 ns for the electric field of 4×10^3 V/m. However, this is a slightly conservative estimate since the electric fields nearer the surface would be somewhat higher (as necessitated by the monotonic Thomas-Fermi distribution), leading to a shorter duration to explosive emission. Besides, the thermal conductivity for copper would likely be lower at the nano-protrusion due to reduced dimensionality. The basic point is that as the characteristic size of

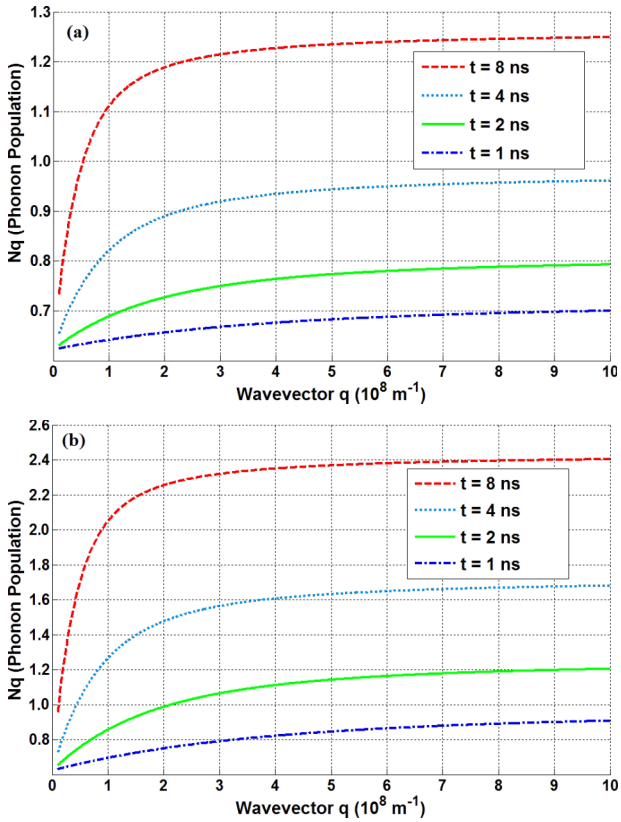

FIG. 1. Phonon population versus wavevector for copper at electric fields of: (a) 2×10^3 V/m, and (b) 4×10^3 V/m.

protrusions is reduced towards nanoscale dimensions, the emitter length-scales begin to get comparable to both the wavelength and mean free path of the heat carriers. This leads to a decrease in the thermal conductivity of the nanostructures compared to their bulk counterparts. In terms of the physics, the reduction occurs for two reasons: (a) Modifications in the phonon dispersion relation, and (b) sharp increases in diffuse interface scattering as the surface-to-volume ratio is enhanced for the nano-protrusions with decreasing dimensions. As a result, depending on the number and sizes of the protrusions at metallic electrodes, one could have a distribution of thermal conductivities. Among these, some sites/protrusions could have sharply reduced values, leading to much faster localized heating and subsequently quicker melting.

In any event, this predicted time scale is roughly in agreement with explosive emission and the observed melting of cathode microtips reported in the literature.[11] Furthermore, since the field magnitudes assumed in these computations correspond to field penetration that is on the order of 0.75 nm into the copper electrode, the melting predicted here would roughly occur over at least the topmost two monolayers of the protrusion.

For completeness, simulation results showing the temperature evolution for electrons and phonons at an electric field of $4x10^3$ V/m are presented in Fig. 3. The $5\times10^7 m^{-1}$ wavevector was chosen for the phonon curve. The results indicate that after starting at room temperature, the values monotonically increase since the electric field is continually applied. As expected, the electron temperatures remains slightly higher those for the phonons. However, a very slow reduction in the temperature difference can be seen.

The above calculations have attempted to present a simplified analysis into the initial development of the explosive emission process. More complex effects such as the ejection of electrons that could produce Freidel oscillations and modify the surface field,[38] or the electric-field guided surface inhomogeneities,[39] would work to further enhance currents. These higher-order effects would lend greater support to our current-driven localized heating scenario.

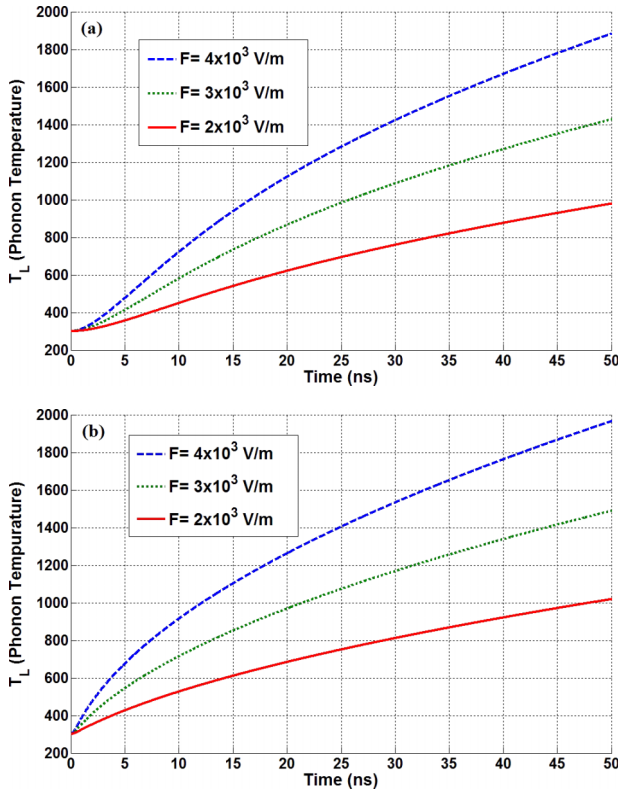

FIG. 2. Phonon temperature versus time for copper cathode at different phonon wavevectors of: (a) $5\times10^7 m^{-1}$, and (b) $10^9\ m^{-1}$.

A single LO phonon mode was used in the calculations. However, the scheme presented here can easily be extended to include the temporal evolution of transverse-phonons in the presence of anharmonic (decay) processes. A simple yet important route to the generation of transverse phonons is through energy relaxation of the longitudinal phonons by spontaneous three-phonon processes. The three-phonon processes would produce two transverse modes with different relaxation rates. This complexity can easily be addressed by having, for example, four instead of two rate equations, but is beyond the present scope. Finally, we have chosen to use simple lumped and constant parameters, such as the value for the decay rate. These parameters could, in general, depend on the local temperature[40] and wavevector values. Furthermore, geometric confinement at

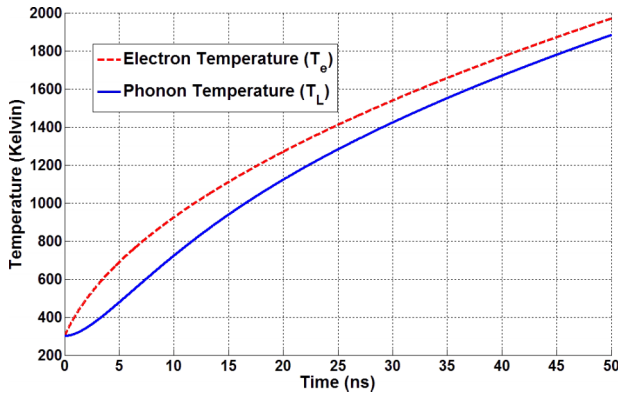

FIG. 3. Simulation results showing the temporal evolution of the temperatures for electrons and ($5\times10^7 m^{-1}$ wavevector) phonons at an electric field of $4x10^3$ V/m.

nano-protrusions would modify the phonon dispersion and shorten phonon mean free paths at the boundaries leading to increased phonon relaxation rates and decreased thermal conductivity.[41] This would hasten the temperature rise and reduce the initiation times for explosive emission. Hence, the present calculations for explosive emission provide a somewhat conservative estimate.

As a final comment, field-assisted evaporation of atoms from a few surface monolayers was first postulated by Müller,[42] and studied more recently based on molecular dynamics simulations for a copper nanotip under high electric fields in the 1-100 GV/m range.[43] These are excessively high field values, which are likely not attainable in actual experiments. However, the synergistic role of heating could allow for explosive emission at much lower electric fields as used in the present analysis. A more subtle aspect concerns the origin of the nano-protrusions which enhance the local electric fields and support a large current. It is possible that Maxwell stress exerted by an external electric field on the metal containing local voids or dissolved gas *near the surface* could lead to plastic deformation and the dynamic formation of surface nano-protrusions. However, the study of this scenario will require detailed molecular dynamics simulations and is beyond the present scope, and will be reported elsewhere.

IV. CONCLUSIONS

The initiation process and time-dependent dynamics of explosive emission from cathodes carrying high current densities was analyzed based on a simple two-temperature, relaxation time model. Such emission has been observed experimentally, and seen to develop over nanosecond time scales. Our results for copper cathodes showed a strong build-up of nonequilibrium phonons. Furthermore, transfer of the kinetic energy gained by the electrons to the phonon system would raise the local lattice temperature to the melting point within about ~ 25 nanoseconds. This timescale is in keeping with experimental observations for the initiation of explosive emission. A logical extension of the model could be atomistic simulations of evaporation at metal nanotips that account for both local heating and the presence of high electric fields in a coupled manner, with inclusion of electromechanical displacements at (or near) the surface.

ACKNOWLEDGEMENTS

The authors acknowledge useful discussions with D. Shiffler (AFRL). The work was supported in part from by the Office of Naval Research under grant N00014-13-1-0567, and by AFOSR grant FA95501010106, "Collaborative Research on Novel High Power Sources for and Physics of Ionospheric Modification".

[1] *High Power Microwaves*, 2nd ed., edited by J. Benford, J. Swegle, and E. Schamiloglu (Taylor and Francis, Boca Raton, 2007).
[2] *High Power Microwave Sources and Technologies*, edited by R. J. Barker and E. Schamiloglu (IEEE Press/John Wiley and Sons, New York, 2001).
[3] R. B. Miller, W. F. McCullough, K. T. Lancaster, and C. A. Muehlenweg, IEEE Trans Plasma Sci. **20**, 332 (1992).
[4] I. Ben-Zvi, Physica C **441**, 21 (2006).
[5] I. Okuda, E. Takahashi, and Y. Owadano, Japanese Journal of Applied Physics, Part 1: Regular Papers and Short Notes and Review Papers **40**, 5407 (2001).
[6] S. Hao, C. Dong, M. Li, X. Zhang, and P. Wu, International Journal of Modern Physics B **23**, 1713 (2009).
[7] X. X. Lin, Y. T. Li, B. C. Liu, F. Du, S. J. Wang, L. M. Chen, L. Zhang, X. L. Liu, J. L. Ma, X. Lu, W. M. Wang, Z. Y. Wei, and J. Zhang, Laser Part. Beams **30**, 39 (2012).
[8] G. Gaertner, J. Vac. Sci. Technol. B **30**, 060801 (2012).
[9] A. Persaud, O. Waldmann, R. Kapadia, K. Takei, A. Javey, and T. Schenkel, Rev. Sci. Instrum. **83**, 02B312 (2012).
[10] G. A. Mesyats, JETP Lett. **7**, 95 (1993).
[11] G. A. Mesyats, Herald of the Russian Academy of Sciences **84**, 242 (2014).
[12] E. Garate, R. MacWilliams, D. Voss, A. Lovesee, K. Hendricks, T. Spencer, M. C. Clark, and A. Fisher, Rev. Sci. Instrum. **66**, 2528 (1995).
[13] R. B. Miller, Journ. Appl. Phys. **84**, 3880 (1998).
[14] S. A. Barengolts, M. Y. Kreindei, and E. A. Litvinov, Surf. Sci. **266**, 126 (1992).
[15] V. G. Pavlov, A. Rabinovish, and V. N. Shrednik, Zh. Tech. Fiz. (In Russian) **45**, 2126 (1975).
[16] V. V. Paranjape and B. V. Paranjape, Phys. Rev. **166**, 757 (1968).
[17] D. G. Cahill, W. K. Ford, K. E. Goodson, G. D. Mahan, A. Majumdar, H. J. Maris, R. Merlin, and S. R. Phillpot, Journ. Appl. Phys. **93**, 793 (2003).

[18] R. Yang, G. Chen, and M. S. Dresselhaus, Nano Letters **5**, 1111 (2005).
[19] G. N. Fursey, M. A. Polyakov, L. A. Shirochin, and A. N. Saveliev, Applied Surface Science **215**, 286 (2003).
[20] A. Anders, *Cathodic Arcs: From Fractal Spots to Energetic Condensation* (Springer-Verlag, New York, 2008).
[21] P. Rumbach and D. B. Go, Journal of Applied Physics **112**, 103302 (2012).
[22] F. B. Hilderbrand, *Advanced Calculus for Applications* (Prentice Hall, Englewood Cliffs, 1962).
[23] R. Miller, Y. Y. Lau, and J. H. Booske, "Electric field distribution on knife-edge field emitters," Appl. Phys. Lett. **91**, 074105 (2007).
[24] A. Majzoobi, R. P. Joshi, A. Neuber, and J. Dickens, "Analysis of cathode emission phenomena: Effects of barrier thinning, field enhancements and local heating," in *Proc. IEEE Pulsed Power Conference*, *Austin, TX*, *2015*, pp. 1-4 (DOI: 10.1109/PPC.2015.7297005).
[25] H. Qiu, R. P. Joshi, A. A. Neuber, and J. C. Dickens, Semiconductor Science and Technology **30**, 105038 (2015).
[26] W. S. Boyle and P. Kisliuk, Phys. Rev. **97**, 255 (1955).
[27] G. Ecker and K. G. Muller, Journ. Appl. Phys. **30**, 1466 (1959).
[28] M. I. Kaganov, I. M. Lifshitz, and L. V. Tanatarov, Sov. Phys. JETP **4**, 173 (1957).
[29] S. I. Anisimov, A. M. Bonch-Bruevich, M. A. El'yashevich, Y. A. Imas, N. A. Pavlenko, and G. R. Romanov, Sov. Phys. Tech. Phys. **11**, 945 (1967).
[30] S. I. Anisimov, B. L. Kapeliovitch, and T. L. Perel'man, Journ. Exp. Theor. Phys. **39**, 375 (1974).
[31] A. Giri, J. T. Gaskins, B. M. Foley, R. Cheaito, and P. E. Hopkins, Journ. Appl. Phys. **117**, 044305 (2015).
[32] A. B. Pippard, "Ultrasonic attenuation in metals," Philos. Mag. **46**, 1104 (1955).
[33] S. Tamura, Phys. Rev. B **31**, 2575 (1985).
[34] J. M. Ziman, *Electrons and Phonons* (Clarendon Press, Oxford, 1960).
[35] R. A. Matula, J. Phys. Chem. Ref. Data **8**, 1147 (1979).
[36] E. Grüneisen, Ann. Phys. **16**, 530 (1933).
[37] F. Bloch, Z. Phys. **59**, 208 (1930).
[38] N. D. Lang and W. Kohn, Phys. Rev. **3**, 1215 (1971).
[39] T. T. Tsong and E. W. Muller, Phys. Rev. **181**, 530 (1969).
[40] R. P. Joshi, P. G. Neudeck, and C. Fazi, Journ. Appl. Phys. **88**, 265 (2000).
[41] E. Chavez-Angel, J. S. Reparaz, J. Gomis-Bresco, M. R. Wagner, J. Cuffe, B. Graczykowski, A. Shchepetov, H. Jiang, M. Prunnila, J. Ahopelto, F. Alzina, and C. M. Sotomayor Torres, APL Materials **2**, 012113 (2014).
[42] E. W. Müller, Phys. Rev. **102**, 618 (1956).
[43] Z. Insepov, J. H. Norem, and A. Hassanein, "Physical Review Special Topics – Accelerators and Beams," **7**, 22001 (2004).